

A simple Monte Carlo method for the calculation of efficiency limit for current-matched tandem solar cells

Abderrahmane Belghachi,
Laboratory of Semiconductor Devices Physics, University of Bechar, Algeria
abelghachi@yahoo.fr

Received 20 Jun 2017; Revised 24 Aug 2017; Accepted 10 Oct 2017

Abstract

Tandem solar cells have demonstrated the potential to increase remarkably the efficiency of solar energy conversion. The widely spread detailed balance principle introduced by Shockley and Queisser 1961 was later applied by De Vos 1980 to tandem structures. Although the mathematical formulation is simple, the mathematical resolution is rather complex and fairly accurate. In this work I describe a simple Monte Carlo (MC) technique to determine the detailed balance limiting efficiency for tandem solar cell stacks. This statistical method uses a simple form of importance sampling scheme adequate for resolving complex equation system depicting a large number of multi-junction without any further approximations. In current-matched tandem solar cells, the band gap of each sub-cell has to be chosen so that the current flowing through each of the sub-cells is the same. The presented results run up to 10 stacked junctions; the algorithm can be applied to a larger number of sub-cells. The simulation is carried out for different conditions; under black body, AM1.5G, AM1.5D spectrums and maximum concentration. The method presented provides a useful tool for researchers to assess the optimum band gap arrangements of current constrained solar cell stacks together with a predicted efficiency limit. The results obtained using this method agrees well with previous calculations.

Keywords: tandem solar cell, high efficiency, Monte Carlo

1. Introduction

Shockley and Queisser (SQ) [1] have first calculated the detailed balance limit efficiency for an ideal solar cell, consisting of the single semiconducting absorber with an energy band-gap E_g . The illumination of a single $p-n$ junction solar cell results in the generation of electron-hole pairs by electronic transition due to fundamental absorption of photons with energies greater than the energy-gap ($h\nu > E_g$), which is a quantum process. The photogenerated pairs either recombine locally or circulate in an external circuit and transmit their energy. The approach reposes on the following main assumptions: *i*)- the probability that a photon, with energy $h\nu > E_g$ incident on the cell surface, will produce a hole-electron pair is equal to unity, while photons of lower energy will produce no effect. *ii*)- all photogenerated electrons and holes thermalize to the band edges (photons with energy greater than E_g produce the same effect). and *iii*)- all photogenerated charge

carriers are collected at short-circuit condition and the upper detailed balance efficiency limit is obtained if radiative recombination is the only allowed recombination mechanism.

For a single junction solar cell, all photons with energies below the bandgap are not absorbed; they will pass through the cell as if it were transparent and had no effect on the energy conversion. Whilst only a certain amount of energy carried by the remaining photons (with energies greater than the gap) contributes to the creation of electron-hole pairs then the extra energy is lost. These two effects, alone, can account for the loss of more than 50% of the solar radiation energy incident on a single junction cell. The limit places maximum solar conversion efficiency around 33.7% assuming a single p - n junction. The best-known example of how to surmount such efficiency restraint is the use of tandem or stacked cells. These sub-cells consist of multiple p - n junctions, each one tuned to a particular energy range of the solar spectrum. The utilization of stacked single junction solar cells operating in tandem is suggested to exceed the performance of one p - n junction solar cell operating alone. The energy bandgap of each sub-cell is tuned to absorb a minute part of the solar spectrum. As the number of solar sub-cells working in a tandem stack tends towards infinity, the upper-limiting efficiency of the stack increases to the absolute theoretical maximum efficiency. This alternative will become increasingly feasible with the possible evolution of materials technology over the decades to 2020 [2,3].

2. Theory

Using the detailed balance principle, in steady state condition, the current density $J(V)$ flowing through an external circuit is the total algebraic rates of electron-hole pairs increase corresponding to the absorption of incoming photons from the sun and surrounding background, in addition to recombination (radiative and non-radiative) [4,5]. This leads to a general current voltage characteristic formula:

$$J(V) = qCf\varphi_s(E_g) + q(1 - Cf)\varphi_a(E_g) - \frac{q}{f_{RR}}\varphi_c(E_g, V) \quad (1)$$

where φ_s , φ_a and φ_c are number of photons emitted, respectively from the sun, ambient atmosphere and the solar cell (converter), per unit area per second within an interval of frequency $d\nu$, with:

$$\varphi_s(E_g) = \left(\frac{2\pi}{c^2}\right) \int_{\nu_g}^{\infty} \frac{v^2 dv}{\exp\left(\frac{h\nu}{kT_s}\right) - 1} \quad (2.a)$$

$$\varphi_a(E_g) = \left(\frac{2\pi}{c^2}\right) \int_{\nu_g}^{\infty} \frac{v^2 dv}{\exp\left(\frac{h\nu}{kT_a}\right) - 1} \quad (2.b)$$

$$\varphi_c(E_g, V) = \left(\frac{2\pi}{c^2}\right) \int_{\nu_g}^{\infty} \frac{v^2 dv}{\exp\left(\frac{h\nu - qV}{kT_c}\right) - 1} \quad (2.c)$$

where T_s , T_a and T_c are the respective temperatures of the sun, ambient background, and solar cell. C and f are respectively, the sun concentration and geometrical factors. f_{RR} represents the fraction of radiative recombination rate or radiative recombination efficiency. If U_{RR} and U_{NR} are radiative and non-radiative recombination rates respectively, f_{RR} is defined as:

$$f_{RR} = \frac{U_{RR}}{U_{RR} + U_{NR}} \quad (3)$$

To determine the efficiency limit of tandem solar cells, the detailed balance principle is applied, in this approach, the limit is taken independently of semiconductor properties except for the band-gap of each single cell. A number of assumptions are necessary in order to calculate the theoretical efficiency.

It is assumed that radiative recombination is the only recombination mechanism; it is also assumed that the sun, ambient and solar cell emits light as black bodies with fluxes given by Planck law of radiation. Sub-cells are arranged in such a way that the sub-cell with the largest band-gap is at the top of the structure, i.e. nearest to incoming radiation and bottom sub-cell has the lowest band-gap ($E_{g,1} > E_{g,2} > E_{g,3} \dots > E_{g,n-1} > E_{g,n}$). Each sub-cell is assumed to absorb all the photons with energies greater than its band-gap. Similarly, each sub-cell is transparent to photons that have energies below its band-gap. Energy selective reflectors are inserted between each pair of sub-cells for optimum performance. Hence, the electrical current crossing the i^{th} sub-cell ($E_{g,i}$) ($i = 2, 3 \dots n-1$) by the detailed balance principle is:

$$J_i(V_i) = qCf\varphi_s(E_{g,i}, E_{g,i-1}) + q(1 - Cf)\varphi_a(E_{g,i}, E_{g,i-1}) - \frac{q}{f_{RR,i}}\varphi_c(E_{g,i}, E_{g,i-1}, V_i) \quad (4)$$

with

$$\varphi_s(E_{g,i}, E_{g,i-1}) = \left(\frac{2\pi}{c^2}\right) \int_{\nu_{g,i}}^{\nu_{g,i-1}} \frac{\nu^2 d\nu}{\exp\left(\frac{h\nu}{kT_s}\right) - 1} \quad (5)$$

$$\varphi_a(E_{g,i}, E_{g,i-1}) = \left(\frac{2\pi}{c^2}\right) \int_{\nu_{g,i}}^{\nu_{g,i-1}} \frac{\nu^2 d\nu}{\exp\left(\frac{h\nu}{kT_a}\right) - 1} \quad (6)$$

and

$$\varphi_c(E_{g,i}, E_{g,i-1}, V_i) = \left(\frac{2\pi}{c^2}\right) \int_{\nu_{g,i}}^{\nu_{g,i-1}} \frac{\nu^2 d\nu}{\exp\left(\frac{h\nu - qV_i}{kT_c}\right) - 1} \quad (7)$$

The topmost sub-cell ($i = 1$) has the same $J(V)$ expression as a single junction (Eq. 1). For the last sub-cell, $i = n$ (bottom sub-cell) upper limit of integration is set to infinity.

The obtained equation system is solved under maximum efficiency conditions for current-matched tandem cells with two conditions: first the power output of each sub-cell should be maximum $P_i = P_{m,i}$, with $P_{m,i} = J_{m,i}V_{m,i}$; second, the maximum current density has to be equal for each sub-cell, $J_{m,i} = J_m$ ($i = 1, 2, 3 \dots n$). With this constrains the solution of a large equation

In Press, Accepted Manuscript – Note to users

system is complicated and necessitates elaborate solving techniques [6-11]. In the present work, I used a numerical based on Monte Carlo statistical technique.

3. Monte Carlo method

Monte Carlo method is a handy tool for simulating systems with many coupled degrees of freedom. In this technique, a large number of points are scattered uniformly over a defined interval as inputs then perform a computation on each point. The method is useful for obtaining numerical solutions to problems too complicated to solve analytically. The most common application of the Monte Carlo method technique is for integration. It is also used to minimize (or maximize) functions of some vector that often has a significant number of dimensions. To obtain accurate solutions, a large number of stochastic events has to be reproduced. Subsequently this leads to an increasing computing time. Several algorithms are suggested to reduce the variance and execution time. A proper sampling technique can improve enormously the performance of a Monte Carlo program. In importance sampling scheme certain values of the random input variables in a simulation have more impact on the parameter being estimated than others. If these "important" values are emphasized by sampling more frequently, then the estimator variance can be reduced.

This paper shows that Monte Carlo technique with a simple form of Importance Sampling scheme is adequate for resolving a complex equation system of a vast number of multi-junction or tandem solar cells without any further approximations. Furthermore, to estimate the photon flux for a black body I used the Incomplete Riemann Zeta Integrals (IRZIs). The energy domain is divided into sub-domains matching the number of stacked cells. Taking a minimum $E_{g,min}$ and a maximum $E_{g,max}$ energy values as limits defining the useful solar spectrum. In this approach, the optimized energy gaps of preceding $(n - 1)$ sub-cells stack are used to obtain sampling domain for the present set of n sub-cells. An optimum value is expected within $\Delta E_{g,i}^n$ range, as shown in a schematic representation of figure 1, where superscript n represents the total number of sub-cells in a stack and subscript i stands for subcell order within the stack ($i = 1, 2 \dots n$).

$$\Delta E_{g,i}^n = E_{g,i-1}^{n-1} - E_{g,i}^{n-1} \quad (i = 2, 3 \dots n-1) \quad (8)$$

$$\Delta E_{g,1}^n = E_{g,max}^{n-1} - E_{g,1}^{n-1} \quad (i = 1) \quad (9)$$

$$\Delta E_{g,n}^n = E_{g,n-1}^{n-1} - E_{g,min}^{n-1} \quad (i = n) \quad (10)$$

In Press, Accepted Manuscript – Note to users

For n tandem cells, firstly a random number r_1 is drawn ($0 < r_1 < 1$) to calculate top most energy gap $E_{g,1}^n$. This is calculated using: $E_{g,1}^n = r_1 \Delta E_{g,1}^n$, then the maximum power point (MPP) for this sub-cell is determined applying the detailed balance principle. The maximum corresponding current density is determined $J_{max,i}^n = J_{max}^n$ and taken as that of the whole stack, as for current matched tandem solar cells. A second random number r_2 is drawn and an energy gap $E_{g,2}^n$ is calculated using equation (8) then $E_{g,2}^n = r_2 \Delta E_{g,2}^n$. After calculating the MPP for this sub-cell, if the maximum current density is very close to J_{max}^n (in our simulation, less than 0.01 % of J_{max}^n is accepted) then a third random number is drawn and so on.

On the contrary, if the sub-cell maximum current density is different from J_{max}^n a second stage is repeated until I find an energy gap that gives a current density of the order of J_{max}^n . The same procedure is carried out again and again until I find all the n energy gaps. Once the n energy gaps are determined I extract a total maximum voltage $V_{max}^n = \sum_{i=1}^n V_{max,i}^n$ and the overall efficiency $\eta = \frac{J_{max}^n V_{max}^n}{P_{in}}$, the same task is repeated several times (N) and different efficiency values, for each set of energy gaps, are obtained. The set of n energy gaps which gives the highest efficiency is retained; obviously optimized energy gaps with a maximum efficiency are reached when N is large.

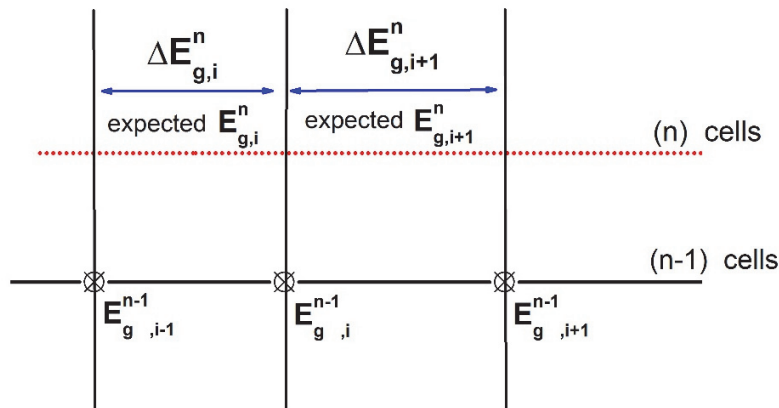


Figure 1: schematic diagram of the sampling energy band-gap segments of each sub-cell (i and $i+1$) of the n stack extracted from the $n-1$ stack.

4. Simulation results and discussion

The first case to be simulated is a single junction cell, taking the expected energy gap between maximum and minimum energy values, $E_{min} = 0.35$ eV and $E_{max} = 3.3$ eV. This simple run is carried out in order to test the program, and find an optimum single energy gap.

In Press, Accepted Manuscript – Note to users

Figure 2 illustrates efficiency against energy band-gap of a solar cell, using different spectrums (AM1.5G AM 1.5 D and black body spectrum at $T_s = 6000^\circ\text{K}$, under both natural and concentrated sunlight). For maximum theoretical efficiency calculation recombination is assumed radiative only ($f_{RR} = 1$) and 100% external fluorescence efficiency, which means that all emitted photons from the cell are allowed to escape [12]. The theoretical maximum efficiency is 45.02% for AM1.5D at highest concentration. Therefore, it can be concluded that in the best of cases, more than 50% of the solar energy is lost because of spectral mismatch, that is; photons with energies below the gap are not absorbed, and the excess energy of absorbed photons with energy higher than the gap is dissipated as heat.

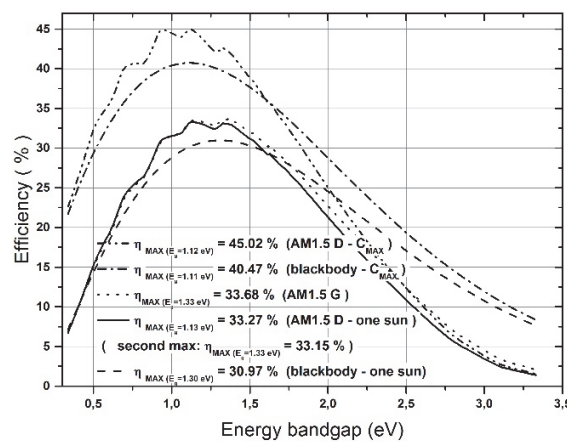
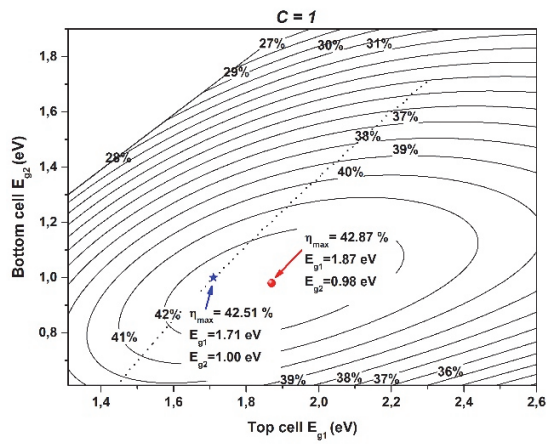
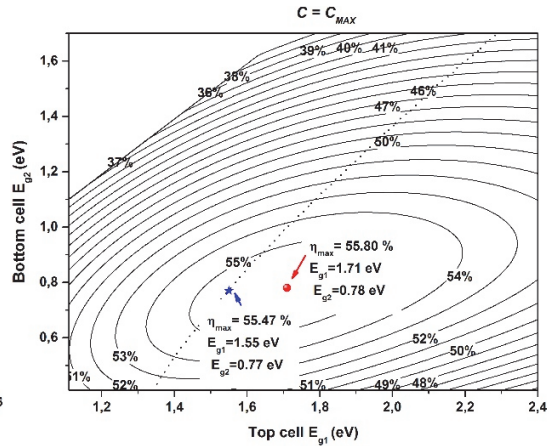


Figure 2: upper limits for single junction solar cell, as a function of band-gap energy for different solar spectrums (black body, AM1.5G, AM1.5D, un-concentrated and concentrated conditions)

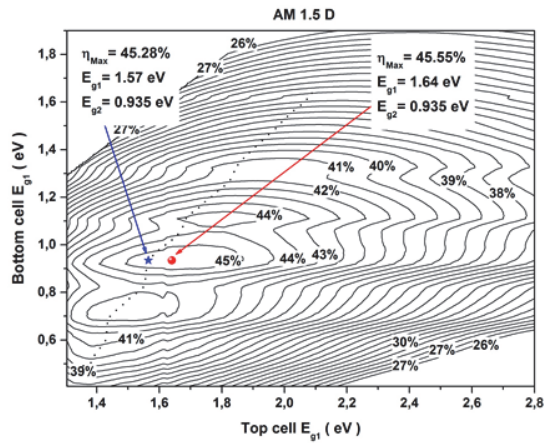
For two tandem solar cells, Monte Carlo technique was applied, and the results are shown in Figure 3. The sample size, number of random numbers, to be drawn is $m \times m$, since for each top sub-cell m bottom sub-cells are needed, this applies to the case of unconstrained tandem stacks where each sub-cell's operating point is independent of others operating points. In the case of constrained tandem stacks for each top sub-cell only one bottom sub-cell verifies the condition of the current match. Thus a shorter calculation time is required. Therefore, as shown in figure 3 unconstrained stacks are represented as contours of equal efficiency, whereas, the constrained ones are gathered in single lines (dotted lines), and the maximum efficiency is slightly lower. The best-obtained results are 60.33% and 60.29% for unconstrained, and series constrained tandem double junction solar cells respectively, under fully concentrated AM1.5 direct solar spectrum (Fig. 3 (d)).



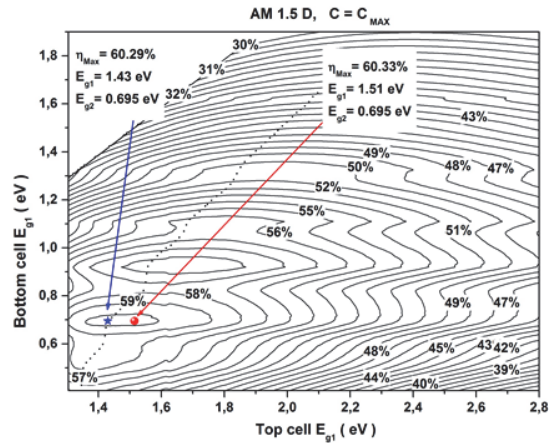
(a)



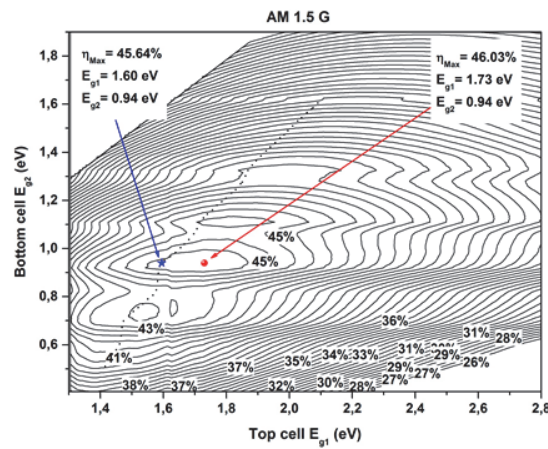
(b)



(c)



(d)



(e)

Figure 3: contour plots of calculated efficiency versus sub-cell band-gaps of unconstrained two-sub-cell tandem for different solar spectrums; panel (a) black body $C = 1$, panel (b) black body $C = C_{max}$, panel (c) AM1.5D, panel (d) maximum concentrated AM1.5D spectrum and panel (e) AM1.5G spectrum. Series constrained two-sub-cell tandems are represented by dotted lines.

The program is run for an increasing number of tandem solar cells, in this algorithm, the optimized energy gaps of preceding $(n-1)$ stack are used as input data to determine importance sampling domains for the following n stack. At the end of each sub-cell calculation, a rejection technique is used, and the calculation restarts from the second sub-cell energy gap when the maximum current density does not match the top sub-cell's current density J_{max}^n . This rejection technique allows an important reduction in computation time (case of constrained series connected stacks). The size of samples is increased to investigate convergence and calculating time. If the size of a sample or sampling number for one sub-cell is m then, total sampling number is $N = m^n$, with n the number of sub-cells in a stack. Figure 4 represents upper efficiencies for a number of sub-cells equal to 2, 4, 6, 8 and 10 versus sampling number of one sub-cell ($m = N^{1/n}$). For a stack of two sub-cells a sample of 50×50 ($m = 50$) is sufficient to saturate (converge) to a constant efficiency value. As the number junctions is increased the required sampling size is increased, to reach about $m = 600$, that is $N = 600^{10}$. We can remark that as the number of sub-cells in a stack is increased the sampling number is increased in order to get to a stable value of the efficiency. As one can see from Fig.4, a value of 10^3 is an acceptable value for a statistical technique and the calculation time is very satisfactory even for a stack of 10 sub-cells.

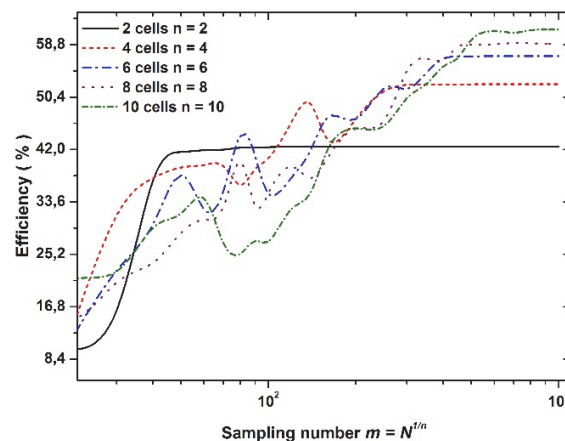


Figure 4: maximum efficiency for series constrained tandem solar stacks versus the sampling size under one sun (black body spectrum), with n sub-cells.

Tables 1 to 5 show the optimum band-gaps, and upper limit efficiencies for series constrained tandem stacks under conditions; black body, AM1.5 global, AM1.5 direct, un-concentrated and

In Press, Accepted Manuscript – Note to users

concentrated radiations. The simulation technique is applied to a number of sub-cells from $n = 1$ to 10, taking a sampling number of $N = 10^{3n}$, this size is very satisfactory up to 10 sub-cells. The obtained results are of the same orders of most published work where more elaborate techniques are used compared to the statistical Monte Carlo method employed in this work. Compared to available literature [6], maximum discrepancy in efficiency for cells up to six junctions is less than 2.55% in the case of AM 1.5 global solar spectrum whereas it is less than 0.7% for black body spectrum.

n	E_{g1}	E_{g2}	E_{g3}	E_{g4}	E_{g5}	E_{g6}	E_{g7}	E_{g8}	E_{g9}	E_{g10}	η (%)
1	1.11	-	-	-	-	-	-	-	-	-	40.74
2	1.45	0.77	-	-	-	-	-	-	-	-	55.46
3	1.82	1.14	0.61	-	-	-	-	-	-	-	63.15
4	2.02	1.39	0.94	0.51	-	-	-	-	-	-	67.88
5	2.17	1.56	1.15	0.79	0.42	-	-	-	-	-	71.08
6	2.31	1.72	1.33	1.02	0.72	0.39	-	-	-	-	73.42
7	2.42	1.85	1.48	1.18	0.92	0.66	0.37	-	-	-	75.17
8	2.51	1.95	1.59	1.30	1.06	0.83	0.60	0.33	-	-	76.55
9	2.60	2.05	1.69	1.42	1.19	0.98	0.77	0.56	0.31	-	77.65
10	2.67	2.12	1.78	1.51	1.29	1.09	0.90	0.71	0.52	0.27	78.55

Table 1: Listing of optimum band-gaps and efficiencies for series constrained tandem stacks, maximum concentration from black body spectrum.

n	E_{g1}	E_{g2}	E_{g3}	E_{g4}	E_{g5}	E_{g6}	E_{g7}	E_{g8}	E_{g9}	E_{g10}	η (%)
1	1.31	-	-	-	-	-	-	-	-	-	30.96
2	1.70	0.98	-	-	-	-	-	-	-	-	42.51
3	1.95	1.29	0.81	-	-	-	-	-	-	-	48.64
4	2.14	1.52	1.10	0.72	-	-	-	-	-	-	52.46
5	2.28	1.69	1.30	0.97	0.65	-	-	-	-	-	55.08
6	2.41	1.83	1.45	1.15	0.88	0.61	-	-	-	-	56.99
7	2.51	1.95	1.59	1.30	1.05	0.82	0.57	-	-	-	58.43
8	2.60	2.05	1.69	1.42	1.18	0.97	0.76	0.54	-	-	59.57
9	2.68	2.13	1.78	1.52	1.29	1.09	0.90	0.71	0.51	-	60.48
10	2.73	2.19	1.85	1.59	1.37	1.18	1.00	0.82	0.65	0.44	61.18

Table 2: Listing of optimum band-gaps and efficiencies for series constrained tandem stacks, under one sun black body spectrum.

n	E_{g1}	E_{g2}	E_{g3}	E_{g4}	E_{g5}	E_{g6}	E_{g7}	E_{g8}	E_{g9}	E_{g10}	η (%)
1	1.33	-	-	-	-	-	-	-	-	-	33.74
2	1.63	0.96	-	-	-	-	-	-	-	-	45.74
3	1.90	1.37	0.94	-	-	-	-	-	-	-	51.57
4	2.00	1.50	1.12	0.72	-	-	-	-	-	-	55.20
5	2.13	1.65	1.30	1.00	0.70	-	-	-	-	-	57.56
6	2.23	1.78	1.46	1.19	0.95	0.69	-	-	-	-	59.51
7	2.32	1.88	1.58	1.35	1.13	0.92	0.66	-	-	-	60.67
8	2.35	1.92	1.63	1.40	1.18	0.97	0.74	0.50	-	-	61.65
9	2.41	2.00	1.72	1.49	1.27	1.12	0.94	0.73	0.50	-	62.50
10	2.47	2.07	1.80	1.58	1.40	1.21	1.04	0.83	0.72	0.49	62.66

Table 3: Listing of optimum band-gaps and efficiencies for series constrained tandem stacks, for an AM1.5 G spectrum.

n	E_{g1}	E_{g2}	E_{g3}	E_{g4}	E_{g5}	E_{g6}	E_{g7}	E_{g8}	E_{g9}	E_{g10}	η (%)
1	1.33	-	-	-	-	-	-	-	-	-	33.15
2	1.57	0.93	-	-	-	-	-	-	-	-	45.29

In Press, Accepted Manuscript – Note to users

- [2] M.A. Green, Third Generation Photovoltaics: Advanced Solar Energy Conversion. In: Springer Series in Photonics 12, Kamiya T., Monemar B., Venghaus H., Yamamoto Y. (Ed.), Springer-Verlag Berlin Heidelberg 2003.
- [3] S. Ahmad, Int. J. Nanoelectronics and Materials 8 (2015) 129-202.
- [4] A. De Vos, J. Phys. D: Appl. Phys., **13** (1980) 839-46.
- [5] P. Baruch, A. De Vos, P. T. Landsberg, J. E. Parrott, Solar Energy Materials and Solar Cells **36** (1995) 201-22.
- [6] A. S. Brown, M. A. Green, Physica E **14** (2002) 96-100.
- [7] F. Meillaud, A. Shah, C. Droz, E. Vallat-Sauvain, C. Miazza, **90**, Issues **18–19** (2006) 2952–59.
- [8] S. P. Bremner, M. Y. Levy, C. B. Honsberg, 22nd European Photovoltaic Solar Energy Conference, 3-7 September 2007, Milan, Italy, 75-78
- [9] A. Marti, G. L. Araujo, Solar Energy Materials and Solar Cells **43** (1996) 203-22
- [10] J. M. Olson, D. J. Friedman S. Kurtz, high-efficiency III-V multijunction solar cells, Handbook of Photovoltaic Science and Engineering, Edited by A. Luke and S. Hegedus, John Wiley & Sons, Ltd, ISBN: 0-471-49196-9 (2003) 359-411.
- [11] S. P. Bremner, M. Y. Levy, C. B. Honsberg, Prog. Photovolt: Res. Appl., **16** (2008) 225– 33
- [12] O. D. Miller, E. Yablonovitch, S. R. Kurtz, IEEE Journal of Photovoltaics **2**, (2012) 303-11